

# Self-Assembly of Antimitotic Peptide at Membranes: Computational and Experimental Investigation

Tanushree Mahata,<sup>†,‡,§</sup> Prasenjit Mondal,<sup>†,§,‡</sup> Debmalya Bhunia,<sup>†</sup> Somen Nandi,<sup>||</sup> Prashant Kurkute,<sup>†</sup> Kankan Bhattacharyya,<sup>\*,†</sup> and Surajit Ghosh<sup>\*,†,§</sup>

<sup>†</sup>Organic & Medicinal Chemistry Division, CSIR-Indian Institute of Chemical Biology, 4, Raja S. C. Mullick Road, Jadavpur, Kolkata 700032, West Bengal, India

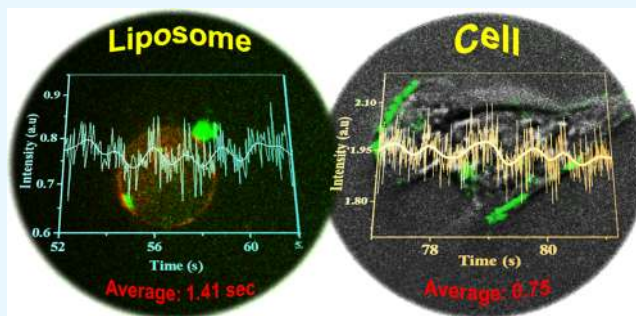
<sup>§</sup>Academy of Scientific and Innovative Research (AcSIR), CSIR-Indian Institute of Chemical Biology Campus, 4 Raja S. C. Mullick Road, Kolkata 700 032, India

<sup>||</sup>Department of Physical Chemistry, Indian Association for the Cultivation of Science, Jadavpur, Kolkata 700032, India

<sup>†</sup>Department of Chemistry, Indian Institute of Science Education & Research Bhopal, Bhopal Bypass Road, Bhauri, Bhopal 462 066, Madhya Pradesh, India

## Supporting Information

**ABSTRACT:** We report the assembly behavior of an antimitotic cell penetrating peptide (CPP) bound with membrane and in solution using experimental and computational techniques. Our study reveals that the antimitotic peptide spontaneously self-assembles and forms a  $\beta$ -sheet-like structure, which is important for cellular entry. Further, we found that this peptide strongly interacts with both liposome membrane and MCF7 membrane. Interestingly, we observed that, during interaction with both lipid membrane and cell membrane, the peptide fluctuates (oscillates) in a similar pattern. The fluctuations in the fluorescence intensity of fluorescein-labeled peptide in the membrane of liposome and cell are attributed to the fluctuation of fluorescein between non-fluorescent neutral form and highly fluorescent dianion form (i.e., prototropic processes). The rate of fluctuation or oscillation is significantly faster at the cell membrane (0.75 s) than that (1.4 s) at the liposome membrane.



## 1. INTRODUCTION

CPPs play a crucial role in cancer therapeutics because of their excellent ability to cross the plasma membrane. Among them, TAT and penetratin are excellent CPPs and studied extensively.<sup>1–3</sup> Interaction between CPPs and membrane depends on the physicochemical nature of both the peptide and membrane.<sup>4</sup> CPPs enter into the cell following two pathways: endocytic pathway and energy-independent pathway,<sup>5,6</sup> where often membrane potential and lipid composition play an important role.<sup>7–12</sup> In this process, the most important factor is the direct interaction of CPPs with membrane lipids during translocation through membrane. The mechanism of these processes involves modification of inverted micelles through electroporation, interaction between phosphate group of membrane and guanidinium group of arginine, and direct translocation through the membrane bilayer.<sup>13–21</sup> Several studies have been performed to understand CPP–membrane interaction during cellular entry. Recently, we found an antimitotic cell-penetrating octapeptide (PR) with single arginine amino acid residue, which can enter into cancer cells through endocytosis process and perturbs intracellular microtubule function.<sup>22</sup> In this manuscript, we investigated

how this PR peptide self-assembles and interacts with lipid membrane during translocation and alters its physical state during interaction with the membrane. We have addressed these using experimental analysis and MD simulation.

## 2. RESULTS AND DISCUSSION

**2.1. Self-Assembly of PR Peptide in Water: Time-Dependent FTIR and CD.** **2.1.1. Time-Dependent FTIR.** Figure 1a–h shows the FTIR spectra of a freshly prepared solution of a PR peptide (10  $\mu$ M) incubated at 37  $^{\circ}$ C in water between 0 and 7 days. For the freshly prepared sample, we found a sharp peak at 1674  $\text{cm}^{-1}$ , which is the characteristic peak of the amide bond. This peak shifts to 1639  $\text{cm}^{-1}$  after one day, indicating the formation of a  $\beta$ -sheet-like structure from day 1, itself. This peak gradually shifts to 1635  $\text{cm}^{-1}$  on the 5th day and does not shift further. This suggests that this peptide self-assembles to form a  $\beta$ -sheet in a time-dependent manner (Figure 1a–h).

Received: July 7, 2018

Accepted: December 25, 2018

Published: January 9, 2019

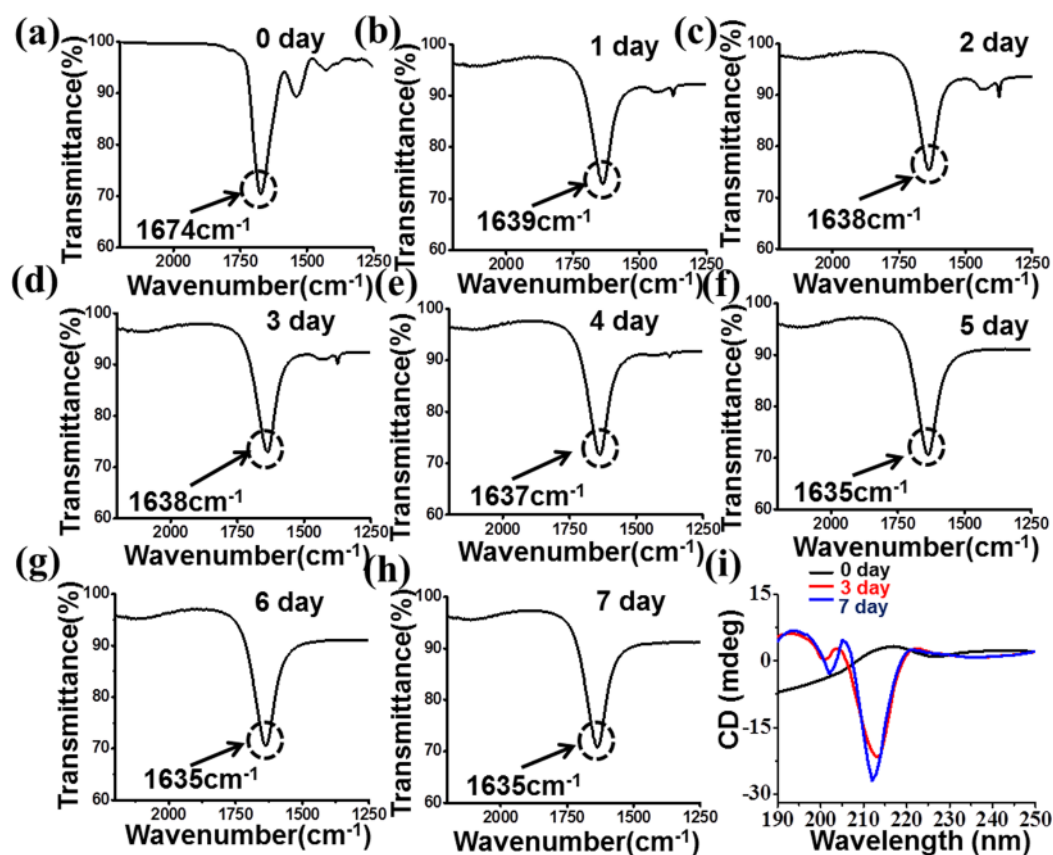


**Figure 1.** (a–h) Day wise (0–7 days) FTIR spectra of PR peptide solution in water, incubated at 37 °C. (i) CD spectra of 0, 3, and 7 day incubated PR peptide solution showing  $\beta$ -sheet structure formation upon self-assembly.

**2.1.2. Time-Dependent CD.** The  $\beta$ -sheet formation of the self-assembled PR peptide observed in FTIR spectroscopy was further confirmed by CD. We have recorded the CD spectra (190–260 nm) of the freshly prepared PR peptide (10  $\mu$ M) solution at 0, 3, and 7 days (Figure 1i). The absence of a peak at 210 nm initially (at 0 day) and its subsequent appearance from 3 to 7 days suggest that the peptide self-assembles to form a  $\beta$ -sheet-like structure (Figure 1i). It has been observed that assembly of peptides has been promoted with increasing incubation time, which results in an increase in ellipticity in CD peak at 210 nm. The appearance of the 210 nm peak in CD spectra and also the shift of amide peak in FTIR towards lower wavenumber clearly indicate that this peptide self-assembles in a time-dependent manner.

**2.2. Interaction of Peptide with Membrane of Reconstituted Liposome and MCF7 Cell: Fluorescence Imaging.** Figure 2 depicts the images of the fluorescein-labeled (green, 488 nm) peptide and reconstituted liposome labeled with TRITC (red, 561 nm). The unilamellar liposomes were reconstituted following the procedure described in our previous publication.<sup>23</sup> From Figure 2a, it is readily seen that the green fluorescein-labeled peptides accumulate at the bilayer membrane region of the liposome. A corresponding bright-field image is shown in Figure 2b, while the 488 nm channel image and a merged image of the bright field and 488 nm channels are shown in Figure S1 (Supporting Information). For better visibility of this peptide lipid membrane interaction, we have performed this study several times. Some of the representative images of the fluorescein–PR peptide’s interaction with the membrane are shown in Figure S2

(Supporting Information). Also, the cross section of one of the liposome is shown in Figure S3 (Supporting Information).

Figure 2c,d describes the interaction of peptide with MCF7. From Figure 2d, it is evident that the green fluorescein-labeled peptide is distributed over the membrane (punctuated images) in some cells and inside some other cells (general green glow). This is because the CPP initially resides at the membrane and eventually enters into the cell. Further, we have performed a co-localization study with fluorescein-attached PR peptide, taking Nile red as the membrane staining dye. We have seen that this dye can stain the membrane lipids rapidly and this peptide is well co-localized with this dye in the membrane region of MCF7 cells (Figure S4, Supporting Information).

These results demonstrate that the PR peptide interacts with the bilayer membrane of the liposome model system as well as with the cellular membrane.

**2.3. Dynamics of Peptide Liposome Membrane and Cellular Membrane.** Dynamics of the fluorescein-labeled peptide at the membrane of liposomes and cell (at punctuated points, Figure 3a) was monitored through the fluctuation of fluorescence intensity of fluorescein, covalently attached with the PR peptide (Figure 3). To verify that the fluctuation is due to interactions with membrane, we did several control experiments.

First, we confirmed that no such fluctuation is observed in the case of the fluorescein-labeled peptide in bulk (buffered water, Figure 3b,c). Thus, the fluctuation is not due to any structural changes inherent in the peptide.

Second, we have captured the confocal images of the peptide bound to the liposome (or the cell membrane, punctuated

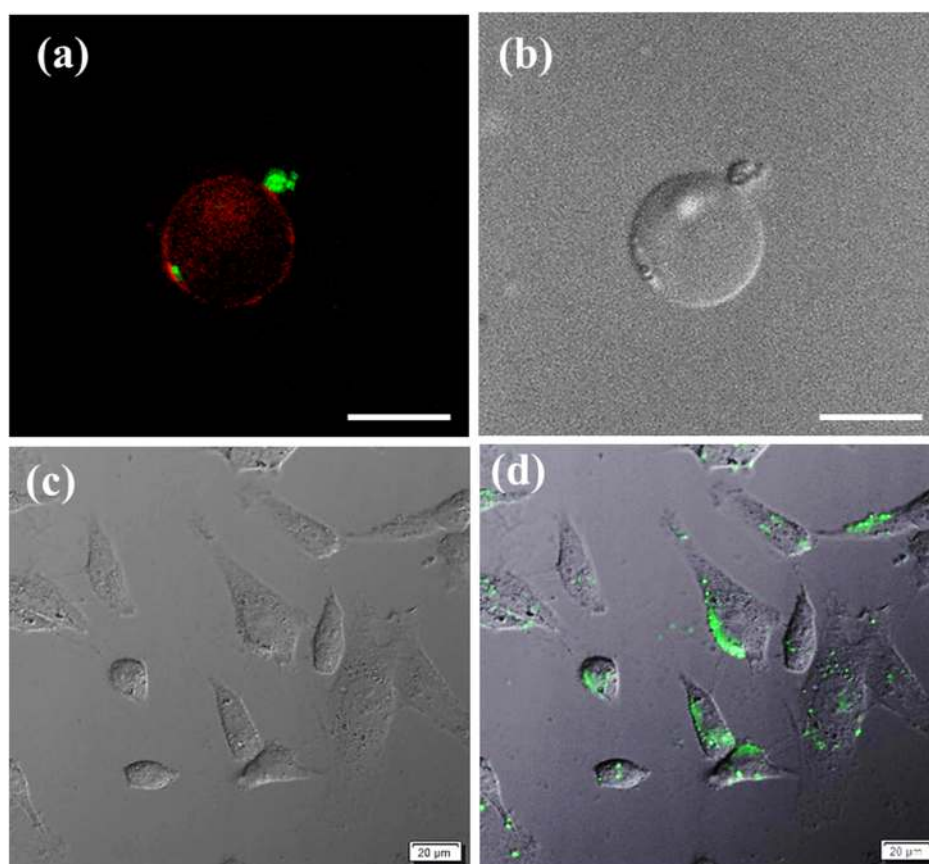


**Figure 2.** Confocal images of interaction of PR peptide with membrane. (a) Merged image (488 and 561 nm channels) of interaction of fluorescein–PR peptide ( $10\ \mu\text{M}$ ) with TRITC-labeled liposome. (b) DIC image of that liposome. (c) Bright-field microscopic image of MCF7 cells. (d) Cellular uptake of fluorescein–PR peptide in 488 nm channel showing accumulation of PR peptide ( $5\ \mu\text{M}$ ) at cellular membrane by incubating the cells for 60 min after treatment.

images, Figure 3a) just before and after recording of each trajectory (Figure S5, Supporting Information). There was no such shift of position of the liposome. Thus, we conclude that the fluctuation in fluorescence intensity is not due to the movement of the liposomes or the cell, on the slide.

Figure 3d shows the intensity versus time traces for fluorescein–PR peptide interacting with the liposome membrane. This trace clearly reveals oscillation in the fluorescence intensity of fluorescein dye attached to PR peptide bound to liposome membrane. A selective portion (52–62 s) of fluorescein trajectory (Figure 3d) is enlarged in Figure 3e. The half-periods of oscillation are obtained by smoothing the trajectory using FFT. The half-periods so obtained for 10 different sets (various positions of the liposome membrane) vary between 1 and 1.7 s, with a mean value of  $1.41 \pm 0.1\ \text{s}$  (Figure 3f).

The fluctuations in the fluorescence intensity of fluorescein-labeled peptide may be attributed to fluctuation of fluorescein between non-fluorescent neutral form and highly fluorescent dianion form (i.e., prototropic processes). Note that the neutral form of fluorescein, which remains inside the membrane, has negligible emission.<sup>24</sup> Fluorescein becomes intensely fluorescent when it is exposed to bulk water and forms a double anion.<sup>24</sup> Further, for control experiment, we have taken a membrane-interacting but nonpenetrating peptide NLRVTEQ and taken the fluorescence fluctuation at the membrane region. We don't find significant fluctuation of this

peptide's membrane interaction (Figure S6, Supporting Information).

In summary, the fluctuation in fluorescence intensity indicates structural fluctuations of the membrane and intermittent location of the fluorescein moiety in a hydrophobic environment (as neutral form) and a hydrophilic region (anion).

Further, in the case of MCF7 cells, we observed similar fluctuations in fluorescence intensity (at the punctuated points of Figure 3a). Figure 3g shows the intensity versus time trajectory of fluorescein–peptide in the cell membrane. The enlarged portion of that trajectory is shown in Figure 3h. Further, smoothing of the trace using FFT is given in Figure 3i. We have recorded the data at 10 different positions of the cellular membrane and calculated the average timescale of oscillation to be  $0.75 \pm 0.1\ \text{s}$ . Some of the representative positions of the fluorescein peptide interaction with MCF7 cell membrane are shown in Figure 3a. The circle represents the positions from where the time traces were recorded (Figure 3a and Figure S5c, Supporting Information). Please note that the circle is only for representation purposes.

It is readily seen that the average timescale of fluctuation in the case of peptide bound to liposome (1.4 s) is nearly two times slower than that (0.75 s) at the cell membrane. This is due to the fact that, during the peptide–liposome interaction, the peptide interacts only with the lipid molecules of liposome. In contrast, in the case the MCF7 cell, the peptide interacts with the cell membrane, which contains apart from lipid

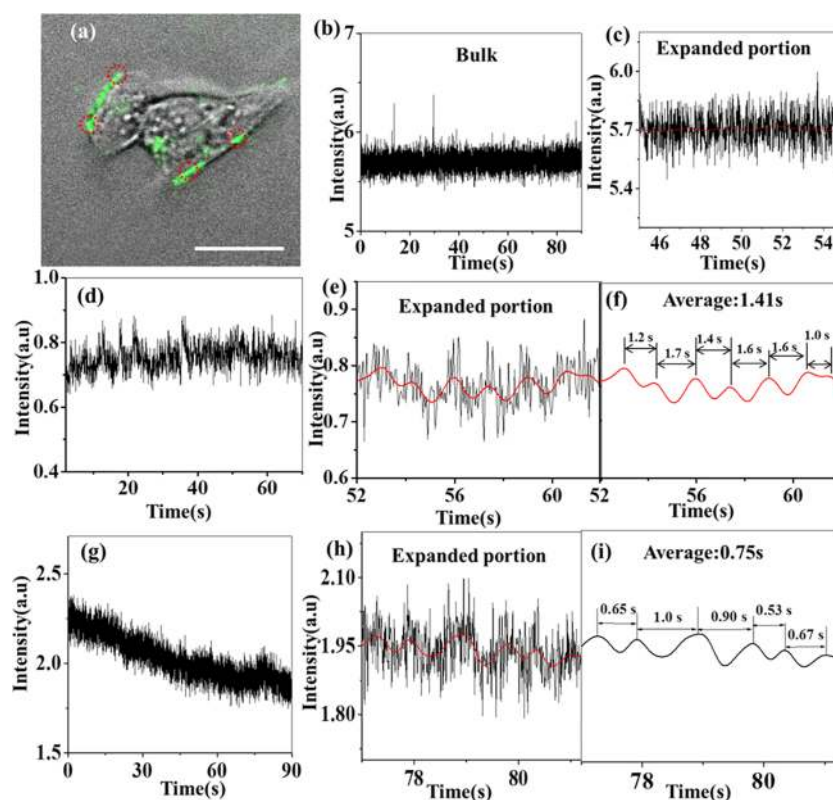


**Figure 3.** (a) Fluctuation of fluorescence intensity signals (oscillations of PR peptide) was recorded from various areas marked in red circles (circles are only for representation purposes). Scale bar corresponds to 20  $\mu\text{m}$ . Fluorescence intensity–time trajectories of fluorescein dye covalently attached to PR peptide in bulk solution at (b) 0–90 s, (c) zoomed portion of (b) (45–55 s). (d) PR peptide interaction with liposome membrane at 0–70 s, (e) zoomed portion of (d) (52–62 s) and (f) smoothed by FFT (showing half-periods). Average time of oscillation is  $1.41 \pm 0.1$  s. The lower panel showing PR peptide interaction with cell membrane at (g) 0–90 s, (h) zoomed portion of (g) (77–81 s), (i) FFT calculation. Average time of oscillation is  $0.75 \pm 0.1$  s.

molecules various membrane-bound receptor proteins. The interactions between the peptide with these complex molecules at the cell membrane may be responsible for the slower timescale of fluctuations.

**2.4. Liposome Leakage Assay To Observe the Fluctuation of Peptide in Lipid Membrane.** To further confirm that the fluctuation of the fluorescence intensity is due to a prototropic process (conversion of fluorescein from the neutral non-fluorescent form to highly fluorescent dianionic form), we performed a leakage assay as the third control experiment. Specifically, we studied the interaction of a liposome labeled non-covalently with fluorescein with the PR peptide (not labeled by fluorescein). The schematic representation and spectral data of liposome leakage assay are shown in Figure 4. It is observed that the emission intensity of fluorescein dye (non-covalently attached to liposome) gradually increases with the increase in the concentration of peptide (Figure S7, Supporting Information). This result clearly indicates that the PR peptide interacts with the lipid membrane and may alter the membrane permeability, which causes release (leakage) of the non-fluorescent form of fluorescein dye (inside lipid membrane) to highly fluorescent anion form (in bulk water).

**2.5. MD Simulation.** It has been documented earlier that the self-assembled peptide, especially  $\beta$ -strand/ $\beta$ -sheet-rich conformation of peptide, facilitates membrane perturbation<sup>23,25,26</sup> and cellular entry. We now applied MD simulation to understand the self-assembly of the PR peptide in solution as well as at the membrane.

**2.5.1. MD Simulation To Study the Self-Assembly of PR Peptide.** Initially, we have performed MD simulation of two PR peptides in solution to understand the atomic details and the nature of assembly of PR peptide. Simulation of two and four molecules of PR peptide has been performed by the following methods (see Experimental; parameters of simulation are given in the Supporting Information), where peptides are separated from each other up to 2 nm in the simulation box, and we ran the simulation for 40 (Figure 5) and 100 ns (Figure S8, Supporting Information). We found that the interactions between the PR peptides are dynamic in the initial stage of simulation. After 10 ns of simulation, two peptides start interacting with each other in parallel orientation. After that, at 20 ns,  $\beta$ -turn-rich structure was observed through H-bonding interactions between alanine, asparagine, and threonine of one molecule with arginine, alanine, and serine of another molecule, respectively (Figure 5b). Interestingly, at 30 ns, they form an antiparallel  $\beta$ -sheet-like structure through strong H-bonding interactions between arginine, alanine, histidine, and serine of one molecule with asparagine, alanine, serine, and histidine of another molecule, respectively (Figure 5c). The secondary structure analysis plot confirms the stability of this  $\beta$ -sheet structure up to 40 ns (Figure 5d and yellow region of Figure 5e, Figure S9, Supporting Information) of simulation of PR peptide. From the simulation study, we have found five key amino acids (alanine, histidine, serine, arginine, and asparagine) in the octapeptide backbone, which are responsible for the formation of this  $\beta$ -sheet structure (Figure 5e, Figure S9, Supporting

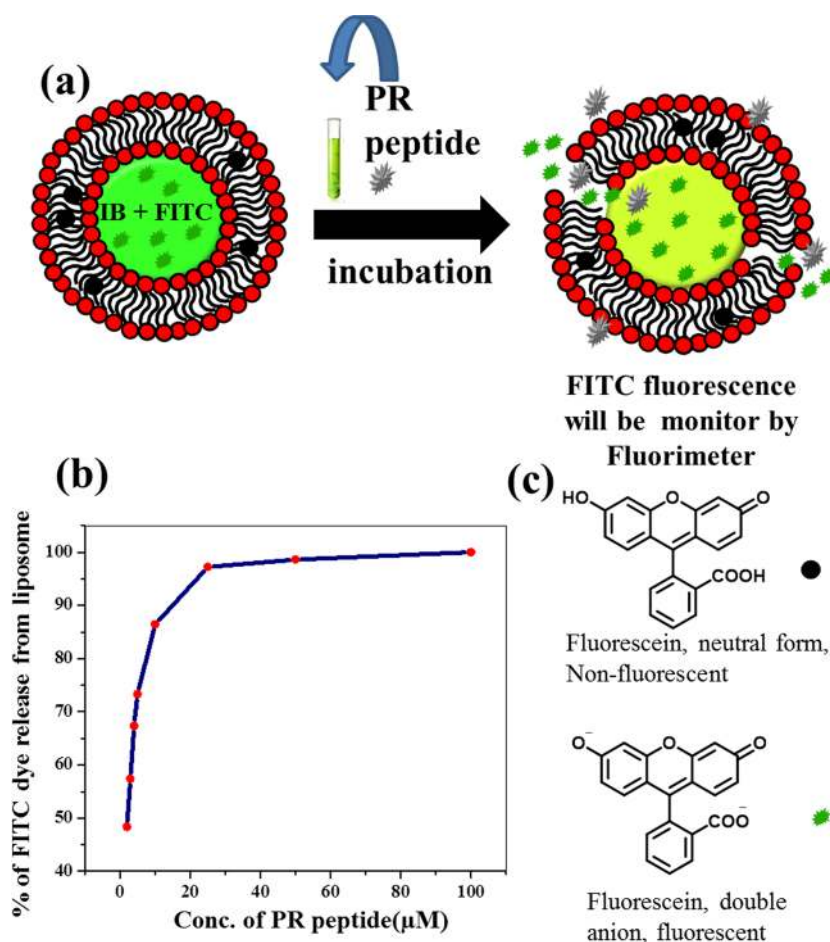


**Figure 4.** (a) Schematic representation of the liposome leakage assay taking PR peptide. (b) Graphical representation shows percent of fluorescein dye release with increasing concentration of PR peptide. (c) Non-fluorescent and fluorescent form of fluorescein.

Information). Also, from the MD simulation movies (Movie S1, Supporting Information), we found that two PR peptides start interacting and form  $\beta$ -turn-like structure and rapidly convert to the  $\beta$ -sheet-rich structure. We found a similar kind of behavior when we ran a MD simulation of four PR molecules for 100 ns. Here, in this case, peptides start interacting after 10 ns, and they form a stable  $\beta$ -sheet-like structure after 30 ns. The secondary structure analysis plot confirms that they form a stable  $\beta$ -sheet structure up to 100 ns of the simulation (Figure S9, Supporting Information). This result clearly indicates that this peptide can adopt the  $\beta$ -sheet structure in solution, which encouraged us to study further the interaction of this peptide with membrane.

**2.5.2. MD Simulation on Peptide Membrane Interaction: Signature of  $\beta$ -Sheet Formation.** In this section, we have carried out a MD simulation with the energy-minimized Berger lipid bilayer, made of 64 DPPC lipid per layer (total 128 lipid molecules) and 9560 water molecules, with three energy-minimized peptides in GROMACS 4.5.5 software for 20 ns. (Detailed parameters of simulation are in the Supporting Information.)

As shown in Figure 6 (Movie S2, Supporting Information), at the liposome bilayer, the peptides start interacting with each other at initial time of the simulation. After that, they interact with the bilayer system with significant affinity and start penetrating into the bilayer system (at 10 ns). These three peptides interact with themselves and the bilayer membrane

throughout the simulation, indicating the strong affinity of the peptide with membrane. Also, we have seen from the MD simulation that the PR peptides indeed form  $\beta$ -sheet-like structure at the lipid membranes by the interaction of alanine, histidine, serine, arginine, and asparagine of PR peptide, which helps to form pore in the bilayer system.

### 3. CONCLUSIONS

In this work, we analyzed in detail the interaction of an antimetabolic peptide with membrane through experiments (time-dependent FTIR, CD, and confocal microscopy) and MD simulation. We have shown that the PR peptides self-assemble in solution and spontaneously form  $\beta$ -sheet structure. Interestingly, in the presence of both liposome and cell membranes, it interacts strongly with both lipid and cell membranes. We found an interesting pattern of alteration of physical states of this peptide while interacting with lipid membrane in both liposome and cell membrane. We show that the fluorescence intensity of fluorescein bound to the peptide fluctuates because of interconversion between the non-fluorescent (neutral) and the fluorescent (dianion) form.<sup>24</sup> Remarkably, the rate of oscillations at the liposome membrane is slower than that at the cell membrane. This difference may be attributed to the difference in the composition of cell membrane and liposome membrane. The cell membrane contains various receptor proteins as additional components. Thus, this report provides new physical insights into the

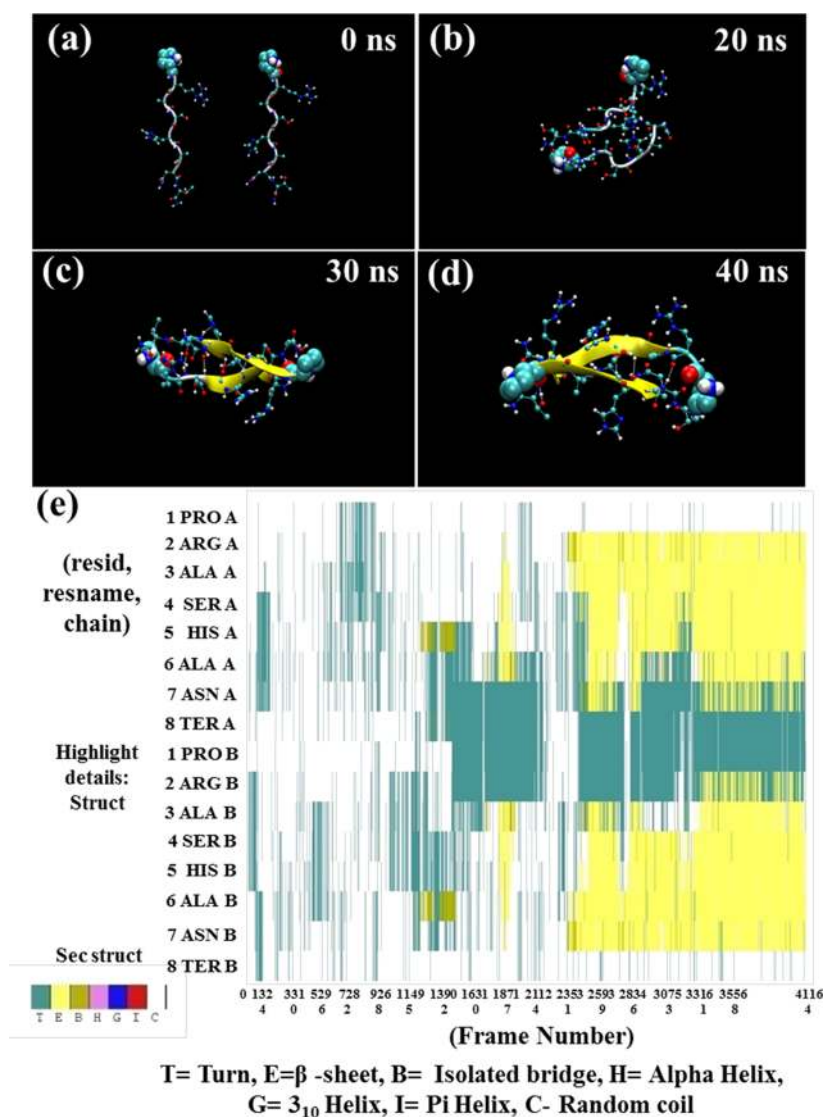


**Figure 5.** Snapshots from a MD simulation movie of two PR peptides at 0 ns (a), at 20 ns forming  $\beta$ -turn-rich structure (b), two peptides assemble rapidly to form antiparallel  $\beta$ -sheet structure at 30 ns (c), stable antiparallel  $\beta$ -sheet structure formation at 40 ns (d). Secondary structure profile diagram of interaction from the MD simulation movie reveals that alanine, histidine, serine, arginine, and asparagine of PR are involved in antiparallel  $\beta$ -sheet structure formation (e).

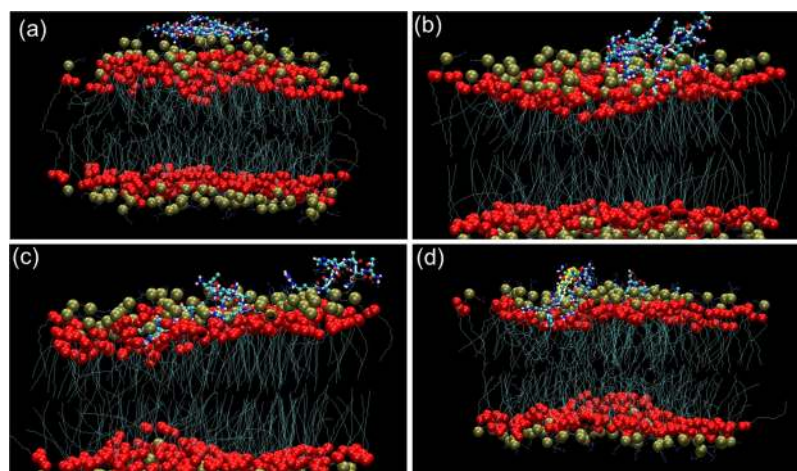


**Figure 6.** Snapshots from the bilayer membrane simulation movie taking three PR peptides at various timescales: (a) 0, (b) 2, (c) 10, and (d) 20 ns.

interaction of an antimetabolic peptide with the cell membrane as well as model liposome.

## 4. EXPERIMENTAL

**4.1. Chemicals.** All the Fmoc amino acids and Rink Amide AM resin were purchased from Merck. Mineral oil, dextran, and BSA were purchased from Sigma-Aldrich. Sucrose was purchased from Sisco Research Laboratory PVT Ltd (SRL). D-Glucose was purchased from Qualigens. NeutrAvidin and diamino poly(ethylene glycol) (PEG 2000) with molecular weight 2000 Da were bought from Invitrogen and Rapp Polymere, respectively. (3-Glycidioxypropyl)trimethoxysilane (GOPTS) was procured from Fluka, and *E,Z*-linked NHS-biotin was from Pierce, Thermo Scientific. NaOH, NaCl, KCl,  $\text{KH}_2\text{PO}_4$ ,  $\text{Na}_2\text{HPO}_4 \cdot 2\text{H}_2\text{O}$ , DMF, hydrogen peroxide (30% solution), and acetone were procured from Merck. Piperidine, DMSO, *O*-(1*H*-benzotriazol-1-yl)-*N,N,N',N'*-tetramethyluronium hexafluorophosphate and diisopropylethylamine were purchased from Spectrochem.  $\text{H}_2\text{SO}_4$  was purchased from Fisher Scientific. Acetonitrile and methanol were purchased from J.T.Baker and Finar, respectively. Catalase and glucose oxidase were generous gifts from Dr. Thomas Surrey's laboratory in EMBL, Heidelberg Germany (currently at London Cancer Research Institute, U.K.). 5(6)-Carboxyfluorescein (fluorescein), kanamycin sulfate, Dulbecco's Modified Eagle's Medium (DMEM), trypsin-EDTA solution, cell culture DMSO,  $\beta$ -casein, and NeutrAvidin were purchased from Sigma Aldrich. Fetal bovine serum (FBS) and penicillin-streptomycin were purchased from Invitrogen. Without further purification, all compounds were used for various experimental purposes.

**4.2. Lipids.** 1,2-Dioleoyl-*sn*-glycero-3-phospho-L-serine sodium salt (DOPS), 1- $\alpha$ -phosphatidylcholine (Egg PC), and 1-palmitoyl-2-oleoyl-*sn*-glycero-3-phospho-(1'-*rac*-glycerol) (sodium salt) (POPG) were purchased from Avanti Polar Lipids. *N*-(Tetramethylrhodamine-6-thiocarbonyl)-1,2-dihexadecanoyl-*sn*-glycero-3-phosphoethanolamine triethylammonium salt (TRITC DHPE) and *N*-(biotinoyl)-1,2-dihexadecanoyl-*sn*-glycero-3-phosphoethanolamine triethylammonium salt (Biotin DHPE) were procured from Invitrogen.

**4.3. Synthesis, Purification, Characterization, and Fluorescein Conjugation with the PR Peptide.** SPPS method was used to synthesize  $\text{NH}_2$ -PRASHANT-CONH<sub>2</sub> (PR) peptide and Fluorescein-PR in a Liberty 1 CEM microwave peptide synthesizer using Rink Amide AM resin. Fluorescein attachment was performed at the N-terminal proline (Pro) moiety of the peptide. We have attached the 5(6)-carboxyfluorescein compound at the N-terminus of the peptide by performing a simple acid-amine coupling reaction using HOBt and DIC in DMF. This crude peptide was purified by reverse-phase HPLC (Shimadzu) and characterized by MALDI-TOF mass spectrometry.<sup>22</sup>

**4.4. MD Simulation of PR Peptide for Studying the Self-Assembly.**<sup>27</sup> MD simulation of two and four PR peptides was performed. Single PR peptide was kept at the center of cubic box solvated by SPC water model. Two and four numbers of Cl atom in 4.5 nm cubic box were used to neutralize the system for two and four peptide's simulation, respectively. Two and four random coil peptides separated by 2.0 nm were solvated by SPC water model. For simulation study, GROMACS version 4.5.5 was used. GROMOS 96 53a6 force field was applied for peptides. Then, the production run

was performed for 40 and 100 ns for two and four peptide's simulation, respectively.

**4.5. PR Peptide Simulation with Membrane.**<sup>28</sup> We have also used GROMACS 4.5.5 software with periodic boundary conditions to study the peptide-membrane interaction. The peptides were placed in a simulation box containing a pre-equilibrated lipid membrane composed of DPPC lipid and water molecules. This lipid membrane was constructed by using 3 PR peptides, 64 DPPC lipids per layer (total 128 lipid), and 9560 water molecules. For long-range electrostatic interaction, particle-mesh Ewald method was used, while Lennard-Jones method was used for short-range repulsive interactions with a cutoff of 1.0 nm. Simulation was performed at a time step of 2 fs. Using V-rescale coupling method, protein and non-protein atoms were coupled to separate coupling baths, and temperature was maintained to 310 K. The pressure of the system was maintained at 1 atm. The force field parameters for the PR peptide, DPPC, and cholesterol molecules were derived from GROMOS 96 53a6 and Berger et al.,<sup>29</sup> respectively. We have performed a 20 ns simulation, after an initial 1 ns of system energy minimization (detailed parameters are in the Supporting Information).

**4.6. FTIR.**<sup>27</sup> We have lyophilized 10  $\mu\text{M}$  freshly prepared and different days incubated PR-peptide solution. FTIR spectroscopy was performed on a PerkinElmer Spectrum 100 FTIR spectrometer using KBr pellets. Spectra of these pellets were recorded with accumulation of 5 times scan and a speed of 0.2  $\text{cm s}^{-1}$  at a resolution of 1.6  $\text{cm}^{-1}$  using a PerkinElmer Spectrum 100 series spectrometer. The LiTaO<sub>3</sub> detector was used for data plotting. To eliminate the interference from air, background correction was also performed for every scan.

**4.7. Time-Dependent CD.** For this experiment, we have prepared a fresh solution of PR peptide (10  $\mu\text{M}$ ) and incubated at 37 °C. Then, CD spectra (190–260 nm) of the freshly prepared, 3, and 7 day incubated solutions were recorded using a JASCO (J-810) spectrometer to observe the secondary structure of PR peptide. The data were analyzed by Origin Pro 8.5 software.

**4.8. Preparation of Physiological Buffer Solution.**<sup>30</sup> Liposome preparation needs two buffer solutions. Internal buffer solution (IB), the buffer solution which was inside the liposome, was prepared by mixing phosphate-buffered saline (PBS 1 $\times$ : 140 mM NaCl, 8.1 mM  $\text{Na}_2\text{HPO}_4 \cdot 2\text{H}_2\text{O}$ , 2.7 mM KCl, and 1.8 mM  $\text{KH}_2\text{PO}_4$  at pH 7.2), 2 M sucrose solution, and dextran solution (400  $\text{mg mL}^{-1}$ ) in MilliQ water. PBS (1 $\times$ ), 20% glucose in water, and BSA solution (100  $\text{mg mL}^{-1}$ ) were mixed to prepare the external buffer (EB), the buffer solution outside the liposome. Osmolarity of EB, EB with fluorescein-PR, and IB was measured by an osmometer, and the osmolarity of the buffers was maintained in such a way that it was 5–10 mOsm less for EB than for IB.

**4.9. Preparation of Lipid-Oil Mixture.**<sup>30</sup> Chloroform solutions of 2.5 mg of Egg PC, 0.5 mg of DOPS, 0.5 mg of POPG, 1% Biotin DHPE, and TRITC DHPE were taken in a 25 mL round bottom flask. Then, the chloroform was evaporated by  $\text{N}_2$  flush followed by high vacuum for 40 min. A thin lipid film was prepared on the inner surface of the round bottom flask. After releasing the vacuum under  $\text{N}_2$ , 5 mL of mineral oil was added to the lipid film in the flask. The flask was then sonicated in cold conditions for 30 min and then incubated in a hot air oven at 50 °C for 3 h. For immobilization of liposome on biotin surface, Biotin DHPE

lipid was used, and for visualization of the membrane of liposome, TRITC DHPE was used.

**4.10. Preparation of Bilayer Liposome.** Mixture A: 200  $\mu\text{L}$  of EB was taken in an Eppendorf tube. Then, 100  $\mu\text{L}$  of TRITC-labeled lipid oil mixture was placed on the top of the EB. The system was placed in an ice bath for 2 h for the formation of a single lipid layer.

Mixture B: 5  $\mu\text{L}$  of IB was added into 600  $\mu\text{L}$  of red and normal lipid–oil mixture. A Hamilton syringe was used to prepare the emulsions, and then the emulsions were incubated at 4  $^{\circ}\text{C}$  for 5 min.

Now, 200  $\mu\text{L}$  of mixture B was placed carefully on the top of mixture A and incubated for 5 min at 4  $^{\circ}\text{C}$ . Then, it was centrifuged for 12 min at the rate 110g, 5 min at the rate 350g, and 3 min at the rate 560g sequentially. The upper oil layer was discarded carefully. The remaining solution was the EB containing liposomes.<sup>30</sup>

**4.11. Preparation of Biotin-Functionalized Surface.**<sup>31</sup> For cleaning, 3M NaOH was used to sonicate the glass coverslips (50  $\times$  50 mm) for 30 min followed by washing with water repeatedly and then treated with piranha solution ( $\text{H}_2\text{O}_2/\text{H}_2\text{SO}_4 = 2:3$ ) for 45 min under sonication. After that, coverslips were cleaned by water and dried with  $\text{N}_2$  stream. For silanization of the glass surfaces, the coverslips were treated with GOPTS for 90 min. Next, the glass surfaces were treated with PEG and heated at 75  $^{\circ}\text{C}$  overnight. Then, careful and repeated washing of the glasses was done with water to remove the excess and unreacted PEG. Finally, the surfaces were treated with NHS-biotin at 75  $^{\circ}\text{C}$  for 1 h. At last, DMF and water were used to wash the biotin-functionalized glass surfaces properly and dried with  $\text{N}_2$  stream.

**4.12. Construction of Flow Chamber and Immobilization of Liposomes.**<sup>30</sup> A flow chamber of 50  $\mu\text{L}$  volume was constructed onto a microscopic glass slide and biotin-functionalized coverslips using double sticky tape (Tesa, Hamburg, Germany). The flow chamber was washed with EB before loading the liposome. Then, neutrAvidin solution containing EB was loaded into the flow chamber and kept for 10 min in that condition. After that, TRITC liposome solution was loaded and washed with EB. After 15 min, we loaded 10  $\mu\text{M}$  fluorescein–PR peptide solution in the flow chamber. After 15 min of incubation, the flow chamber was washed two times with EB and sealed. Finally, the flow chamber was ready for microscopic images and other studies.

**4.13. Preparation of Liposome and Entrapment of Dye for Leakage Assay.** We have mixed chloroform solutions of DOPC, cholesterol, and 5(6)-carboxyfluorescein dye in a ratio of 4:1:1 for the preparation of fluorescein dye encapsulated liposome. Then, the mixed chloroform solutions of all the components were taken in a glass vial, and it was evaporated by nitrogen flash, dried under vacuum, and hydrated overnight at 4  $^{\circ}\text{C}$ . For the formation of multilamellar liposomes (MLLs), the hydrated solution was then vortexed for 2–3 min. MLLs were then sonicated for 5 min followed by probe sonication under ice-cold conditions. Next, it was centrifuged at 5000 rpm for 30 min to remove free fluorescein dye. Then, we passed the solution through Sephadex-40 column and collected the different fractions of eluent. Concentration of encapsulated fluorescein was measured by taking the absorbance of different fractions using a UV spectrophotometer (Cary 60 UV–vis, Agilent Technologies). The fraction having maximum absorbance value, that is,

fluorescein-encapsulated liposome, was used for further studies.<sup>32</sup>

The fraction having maximum absorbance value is 0.69 a.u. Now, from Lambert–Beer's law, we know

$$A = \epsilon \times c \times l \quad (1)$$

where  $A$  is the absorbance,  $C$  is the concentration,  $\epsilon$  is the molar extinction coefficient, and  $l$  is the path length. The molar extinction coefficient ( $\epsilon$ ) for fluorescein dye is 70000  $\text{M}^{-1} \text{cm}^{-1}$ . So, the calculated concentration for encapsulated fluorescein dye is 9.85  $\mu\text{M}$ .

**4.14. Cell Culture.** MCF7 cells were purchased from National Centre for Cell Science, Pune, India. Cells were cultured in a 5%  $\text{CO}_2$  incubator at 37  $^{\circ}\text{C}$  using DMEM having 10% FBS, penicillin (50 units/mL), kanamycin sulfate (110  $\mu\text{g L}^{-1}$ ), and streptomycin (50  $\mu\text{g mL}^{-1}$ ). For cell detachment, trypsin–EDTA (1 $\times$ ) solution was used.

**4.15. Images of Interaction between PR Peptide and Membrane Was Captured Using a Fluorescence Microscope.**<sup>22</sup> Prior to treatment, MCF7 cells were harvested overnight in DMEM comprising 10% FBS on a cover glass bottom dish. Cells were treated with fluorescein–PR peptide solution for 60 min. After that, it was washed with PBS. Then, colorless serum-free medium was used to wash the cells. Finally, the coverslip was ready for the microscopic imaging.

For co-localization study, we follow the similar method as described earlier, cells were first treated with a membrane staining dye Nile red<sup>33</sup> (100 nM) and incubated for 20 min. Afterward, cells were washed with PBS, treated with 5  $\mu\text{M}$  fluorescein–PR peptide, and incubated for 30 min. Then, the cells were first washed with PBS and finally with colorless serum-free medium. Cell imaging was done by using a fluorescence microscope (Olympus IX83) equipped with an Andor iXon3 897 electron multiplying charged-coupled device (EMCCD) camera.

**4.16. Confocal Microscopy.** Our confocal microscope's (PicoQuant, MicroTime 200) detailed setup was described earlier.<sup>34–36</sup> To record the emission spectra, an EMCCD attached to a spectrograph (Andor Technology, Shamrock series) was used in the confocal microscope. The fluorescence was focused through a pinhole before entering into the two detectors. All experiments were executed at room temperature.

**4.17. Leakage Assay.** The liposome solution having maximum fluorescein absorption was mixed with PR peptide in a glass vial. The absorption value of this solution was then monitored at 485 nm with increasing concentration (2–100  $\mu\text{M}$ ) of PR peptide. The increase in the fluorescence intensity of fluorescein indicates disruption of liposome membrane and release of fluorescein dye from the liposomes.<sup>37</sup> Note that the neutral form of fluorescein, which remains inside the membrane, has negligible emission. Fluorescein becomes intensely fluorescent when it is released in bulk water and forms a double anion.<sup>24</sup>

**4.18. Data Analysis.** Microscopic images were processed by Nikon NIS Ar software and ImageJ software. Origin Pro 8.5 software was used to evaluate the spectroscopic data and statistical analysis.

## ■ ASSOCIATED CONTENT

### 📄 Supporting Information

The Supporting Information is available free of charge on the ACS Publications website at DOI: 10.1021/acsomega.8b01568.



MD simulation of 2 and 4 PR peptide, PR peptide interactions with lipid and cellular membrane (PDF)  
MD simulation of two PR peptides for 40 ns (MPG)  
MD simulation PR peptide interaction with lipid membrane for 20 ns (MPG)

## AUTHOR INFORMATION

### Corresponding Authors

\*E-mail: [kankan@iiserb.ac.in](mailto:kankan@iiserb.ac.in) (K.B.).

\*E-mail: [sghosh@iicb.res.in](mailto:sghosh@iicb.res.in) (S.G.). Fax: +91-33-2473-5197/0284. Tel: +91-33-2499-5872.

### ORCID

Tanushree Mahata: 0000-0002-7417-0470

Prasenjit Mondal: 0000-0003-0767-449X

Debmalya Bhunia: 0000-0001-8649-0466

Somen Nandi: 0000-0001-8484-761X

Kankan Bhattacharyya: 0000-0002-7463-3156

Surajit Ghosh: 0000-0002-8203-8613

### Author Contributions

T.M. and P.M. synthesized and purified the peptide and performed various in vitro assays and helped S.G. in writing the manuscript. D.B. helped T.M. and P.M. in various experiments. P.M. and S.N. performed fluctuation studies using the confocal microscope. P.K. performed MD simulation of peptide membrane interaction. S.G. and K.B. conceived the idea, supervised the project, and wrote the manuscript.

### Author Contributions

‡T.M. and P.M. contributed equally.

### Notes

The authors declare no competing financial interest.

## ACKNOWLEDGMENTS

T.M., P.M., S.N., and P.K. thanks CSIR for awarding their fellowships. D.B. thanks the DST-Inspire fellowship. K.B. thanks the JC Bose fellowship. S.G. kindly acknowledges SERB, India (EMR/2015/002230) for financial assistance.

## ABBREVIATIONS

CPPs, Cell-penetrating peptides; MCF7 cell, Human breast cancer cell; SPPS, Solid-phase peptide synthesis; SPC, Simple point charge; MD, Molecular dynamics

## REFERENCES

- (1) Joliot, A.; Pernelle, C.; Deagostini-Bazin, H.; Prochiantz, A. Antennapedia Homeobox Peptide Regulates Neural Morphogenesis. *Proc. Natl. Acad. Sci. U. S. A.* **1991**, *88*, 1864–1868.
- (2) Perez, F.; Lledo, P. M.; Karagozeos, D.; Vincent, J. D.; Prochiantz, A.; Ayala, J. Rab3A and Rab3B Carboxy-terminal Peptides are both Potent and Specific Inhibitors of Prolactin Release by Rat Cultured Anterior Pituitary cells. *Mol. Endocrinol.* **1994**, *8*, 1278–1287.
- (3) Derossi, D.; Joliot, A. H.; Chassaing, G.; Prochiantz, A. The Third Helix of the Antennapedia Homeodomain Translocates Through Biological Membranes. *J. Biol. Chem.* **1994**, *269*, 10444–10450.
- (4) Ziegler, A. Thermodynamic Studies and Binding Mechanisms of Cell-penetrating Peptides with Lipids and Glycosaminoglycans. *Adv. Drug Delivery Rev.* **2008**, *60*, 580–597.
- (5) Drin, G.; Cottin, S.; Blanc, E.; Rees, A.R.; Temsamani, J. Studies on the Internalization Mechanism of Cationic Cell-penetrating Peptides. *J. Biol. Chem.* **2003**, *278*, 31192–31201.
- (6) Ott, M.; Shai, Y.; Haran, G. Single-Particle Tracking Reveals Switching of the HIV Fusion Peptide between Two Diffusive Modes in Membranes. *J. Phys. Chem. B* **2013**, *117*, 13308–13321.
- (7) Terrone, D.; Sang, S. L. W.; Roudaia, L.; Silvius, J. R. Penetratin and Related Cell-penetrating Cationic Peptides can Translocate across Lipid Bilayers in the Presence of a Transbilayer Potential. *Biochemistry* **2003**, *42*, 13787–13799.
- (8) Magzoub, M.; Pramanik, A.; Graslund, A. Modeling the Endosomal Escape of Cell-penetrating Peptides: Transmembrane pH Gradient Driven Translocation across Phospholipid Bilayers. *Biochemistry* **2005**, *44*, 14890–14897.
- (9) Madani, F.; Peralvarez-Marín, A.; Graslund, A. Liposome Model Systems to Study the Endosomal Escape of Cell-Penetrating Peptides: Transport across Phospholipid Membranes Induced by a Proton Gradient. *J. Drug Delivery* **2011**, *2011*, 897592.
- (10) Sasmal, D. K.; Yadav, R.; Lu, H. P. Single-Molecule Patch-Clamp FRET Anisotropy Microscopy Studies of NMDA Receptor Ion Channel Activation and Deactivation under Agonist Ligand Binding in Living Cells. *J. Am. Chem. Soc.* **2016**, *138*, 8789–8801.
- (11) Swiecicki, J. M.; Bartsch, A.; Tailhades, J.; Di Pisa, M.; Heller, B.; Chassaing, G.; Mansuy, C.; Burlina, F.; Lavielle, S. The Efficacies of Cell-penetrating Peptides in Accumulating in Large Unilamellar Vesicles Depend on Their Ability to Form Inverted Micelles. *ChemBioChem* **2014**, *15*, 884–891.
- (12) Thoren, P. E. G.; Persson, D.; Karlsson, M.; Norden, B. The Antennapedia Peptide Penetratin Translocates across Lipid bilayers - The First Direct Observation. *FEBS Lett.* **2000**, *482*, 265–268.
- (13) Binder, H.; Lindblom, G. Charge-dependent Translocation of the Trojan Peptide Penetratin across Lipid Membranes. *Biophys. J.* **2003**, *85*, 982–995.
- (14) Rothbard, J. B.; Jessop, T. C.; Lewis, R. S.; Murray, B. A.; Wender, P. A. Role of Membrane Potential and Hydrogen Bonding in the Mechanism of Translocation of Guanidinium-rich Peptides into Cells. *J. Am. Chem. Soc.* **2004**, *126*, 9506–9507.
- (15) Verma, R.; Malik, C.; Azmi, S.; Srivastava, S.; Ghosh, S.; Ghosh, J. K. A Synthetic S6 Segment Derived from KvAP Channel Self-assembles, Permeabilizes Lipid Vesicles, and Exhibits Ion Channel Activity in Bilayer Lipid Membrane. *J. Biol. Chem.* **2011**, *286*, 24828–24841.
- (16) Su, Y.; Mani, R.; Hong, M. Asymmetric Insertion of Membrane Proteins in Lipid Bilayers by Solid-state NMR Paramagnetic Relaxation Enhancement: A Cell-penetrating Peptide Example. *J. Am. Chem. Soc.* **2008**, *130*, 8856–8864.
- (17) Dietz, G. P. H.; Bahr, M. Delivery of Bioactive Molecules into the Cell: The Trojan Horse Approach. *Mol. Cell. Neurosci.* **2004**, *27*, 85–131.
- (18) Fischer, R.; Fotin-Mleczek, M.; Hufnagel, H.; Brock, R. Break on through to the Other Side—Biophysics and Cell Biology Shed Light on Cell-Penetrating Peptides. *ChemBioChem* **2005**, *6*, 2126–2142.
- (19) Mae, M.; Langel, U. Cell-penetrating Peptides as Vectors for Peptide, Protein and Oligonucleotide Delivery. *Curr. Opin. Pharmacol.* **2006**, *6*, 509–514.
- (20) Murriel, C. L.; Dowdy, S. F. Influence of Protein Transduction Domains on Intracellular Delivery of Macromolecules. *Expert Opin. Drug. Deliv.* **2006**, *3*, 739–746.
- (21) Di Pisa, M.; Chassaing, G.; Swiecicki, J. M. Translocation Mechanism(s) of Cell-penetrating Peptides: Biophysical Studies using Artificial Membrane Bilayers. *Biochemistry* **2015**, *54*, 194–207.
- (22) Bhunia, D.; Mohapatra, S.; Kurkute, P.; Ghosh, S.; Jana, B.; Mondal, P.; Saha, A.; Das, G.; Ghosh, S. Novel Tubulin-targeted Cell penetrating Antimitotic Octapeptide. *Chem. Commun.* **2016**, *52*, 12657–12660.
- (23) Salay, L. C.; Qi, W.; Keshet, B.; Tamm, L. K.; Fernandez, E. J. Membrane Interactions of a Self-assembling Model Peptide that Mimics the Self-association, Structure and Toxicity of Abeta(1-40). *Biochim. Biophys. Acta* **2009**, *1788*, 1714–1721.

(24) Sjoback, R.; Nygren, J.; Kubista, M. Absorption and Fluorescence Properties of Fluorescein. *Spectrochim. Acta A* **1995**, *51*, L7–L21.

(25) de Planque, M. R. R.; Raussens, V.; Contera, S. A.; Rijkers, D. T. S.; Liskamp, R. M. J.; Ruysschaert, J.-M.; Ryan, J. F.; Separovic, F.; Watts, A.  $\beta$ -Sheet Structured  $\beta$ -Amyloid(1-40) Perturbs Phosphatidylcholine Model Membranes. *J. Mol. Biol.* **2007**, *368*, 982–997.

(26) Yao, H.; Lee, M. W.; Waring, A. J.; Wong, G. C. L.; Hong, M. Viral Fusion Protein Transmembrane Domain Adopts  $\beta$ -strand Structure to Facilitate Membrane Topological Changes for Virus-cell Fusion. *Proc. Natl. Acad. Sci. U. S. A.* **2015**, *112*, 10926–10931.

(27) Biswas, A.; Kurkute, P.; Jana, B.; Laskar, A.; Ghosh, S. An Amyloid Inhibitor Octapeptide forms Amyloid Type Fibrous Aggregates and Affects in Microtubule Motility. *Chem. Commun.* **2014**, *50*, 2604–2607.

(28) Khandelia, H.; Ipsen, J. H.; Mouritsen, O. G. The impact of peptides on lipid membranes. *Biochim. Biophys. Acta* **2008**, *1778*, 1528–1536.

(29) Berger, O.; Edholm, O.; Jahnig, F. Molecular dynamics simulations of a fluid bilayer of dipalmitoylphosphatidylcholine at full hydration, constant pressure, and constant temperature. *Biophys. J.* **1997**, *72*, 2002–2013.

(30) Saha, A.; Mondal, G.; Biswas, A.; Chakraborty, I.; Jana, B.; Ghosh, S. In vitro Reconstitution of a Cell-like Environment using Liposomes for Amyloid beta Peptide Aggregation and Its Propagation. *Chem. Commun.* **2013**, *49*, 6119–6121.

(31) Biswas, A.; Saha, A.; Jana, B.; Kurkute, P.; Mondal, G.; Ghosh, S. A Biotin Micropatterned Surface Generated by Photodestruction Serves as a Novel Platform for Microtubule Organisation and DNA Hybridisation. *ChemBioChem* **2013**, *14*, 689–694.

(32) Bhunia, D.; Saha, A.; Adak, A.; Das, G.; Ghosh, S. A Dual Functional Liposome Specifically Targets Melanoma Cells through Integrin and Ephrin Receptors. *RSC Adv.* **2016**, *6*, 113487–113491.

(33) Gao, F.; Mei, E.; Lim, M.; Hochstrasser, R. M. Probing Lipid Vesicles by Bimolecular Association and Dissociation Trajectories of Single Molecules. *J. Am. Chem. Soc.* **2006**, *128*, 4814–4822.

(34) Chowdhury, R.; Nandi, S.; Halder, R.; Jana, B.; Bhattacharyya, K. Structural relaxation of acridine orange dimer in bulk water and inside a single live lung cell. *J. Chem. Phys.* **2016**, *144*, 065101.

(35) Nandi, S.; Mondal, P.; Chowdhury, R.; Saha, A.; Ghosh, S.; Bhattacharyya, K. Amyloid beta peptides inside a reconstituted cell-like liposome system: aggregation, FRET, fluorescence oscillations and solvation dynamics. *Phys. Chem. Chem. Phys.* **2016**, *18*, 30444–30451.

(36) Nandi, S.; Parui, S.; Jana, B.; Bhattacharyya, K. Local Environment of Organic Dyes in an Ionic Liquid–Water Mixture: FCS and MD Simulation. *J. Chem. Phys.* **2018**, *149*, 054501.

(37) Rajasekhar, K.; Madhu, C.; Govindaraju, T. Natural Tripeptide-Based Inhibitor of Multifaceted Amyloid  $\beta$  Toxicity. *ACS Chem. Neurosci.* **2016**, *7*, 1300–1310.